ELSEVIER

Journal of Photochemistry and Photobiology A: Chemistry 99 (1996) 165–175

Journal of PHOTOCHEMISTRY AND PHOTOBIOLOGY A:CHEMISTRY

Enhanced excitation energy transfer in microdroplets — a study by time-resolved fluorescence microscopy

Krishna K. Pandey [1], Satoshi Hirayama *

Laboratory of Chemistry, Kyoto Institute of Technology, Matsugasaki, Sakyo-ku, Kyoto 606 Japan

Received 5 February 1996; accepted 29 April 1996

Abstract

Time-resolved fluorescence microscopy was used to study the fluorescence quenching of rhodamine 6G (R6G) in single microdroplets with diameters equal to or larger than 2 μm. The microdroplets were prepared by dispersing ethylene glycol solutions of R6G in silicone oil. The fluorescence lifetime of R6G was found to be independent of the size of the droplet at low concentrations (1.0×10^{-4} M or less); a value of 3.60 ± 0.02 ns was observed, which was measured for the bulk solution in a thin glass capillary, indicating that neither the radiative process nor the intramolecular radiationless processes of R6G were influenced by the size of the droplet for droplets greater than 2 μm in diameter. However, a significant size effect on the fluorescence decay was observed at higher concentrations of R6G. At the highest concentration of R6G (5.2×10^{-3} M) examined in this work, the apparent fluorescence lifetime decreased from 3.60 ± 0.02 ns for droplets larger than 20 μm in diameter to approximately 0.4 ± 0.07 ns for the smallest droplet of 2 μm in diameter. Despite such a significant decrease in the fluorescence lifetime, the decay curves could be analysed satisfactorily by fitting to single exponential functions. When malachite green (MG) was added as an acceptor to a solution of R6G (10^{-4} M), a large enhancement of Förster-type energy transfer from R6G to MG, as compared with the bulk solution, was observed for droplets with diameters of less than 10 μm. In this case, all the decay curves obtained were well described by the function derived from the Förster-type energy transfer, but the effective critical distance increased by approximately a factor of two on going from a 10 μm droplet to a 2 μm droplet. On the other hand, the fluorescence quenching of R6G by potassium iodide (KI) showed only a small size effect on the quenching rate constant. The significant size effect observed for droplets of concentrated R6G solution can be interpreted in terms of enhanced Förster-type energy migration, followed by energy trapping by dimers of R6G which act as quenching centres.

Keywords: Enhanced energy transfer; Malachite green; Microdroplet, Morphology-dependent resonance; Radiative lifetime; Rhodamine 6G; Size effect; Time-resolved fluorescence microscopy

1. Introduction

Quenching of the fluorescence of molecules in condensed media has been the subject of numerous investigations. This is a powerful technique for solving diverse problems in physical, chemical and biological science. Although extensive investigations have been performed on fluorescence characteristics under various conditions in bulk solutions, fluorescence studies on aerosols or microdroplets have been rather limited [1]. This is presumably because stable microdroplets are difficult to prepare [2], and the total fluorescence intensity from a single droplet or even from an ensemble of droplets, such as a mist, is very low compared with that from the bulk solution. With the availability of lasers as excitation source and/or the introduction of a fluorescence microscope, such studies are now possible. Some work on fluorescence quenching in aerosols or microdroplets has appeared in the literature [1,3–14]. However, most of these investigations have been limited to steady state measurements. Campillo and Lin [1] examined the non-radiative energy transfer from rhodamine 6G (R6G) to cresyl violet in bulk solution and in a droplet of 40 μm in diameter, and found excellent agreement between the energy transfer characteristics in the bulk solution and aerosols [1]. Recently, Folan et al. [4] have investigated the energy transfer from coumarin (donor) to R6G (acceptor) in a glycerol host droplet of 10 μm in diameter. They observed a large increase in the ratio of the acceptor to the donor fluorescence quantum yield over that measured in bulk solution and explained the observed enhancement in energy transfer in the droplet as being due to the interaction

* Corresponding author. Tel.: +81 75 724 7743; fax: +81 75 724 7710; e-mail: satoshi@ipc.kit.ac.jp

[1] Present address: Institute of Wood Science and Technology, P.O. Malleswaram, Bangalore 560003, India.

PII S1010-6030(96)04394-8

of the acceptor and donor dipoles with the surface resonance modes [4]. While the energy transfer was reported to be enhanced by about two orders of magnitude relative to the usual Förster-type energy transfer seen in the bulk medium, the rate of energy transfer was found to be independent of the acceptor concentration above 10^{-6} M [4]. Following this experiment, Druger et al. [8] presented a theory to explain the enhanced energy transfer expected in dielectric microdroplets. Related to enhanced energy transfer, Barnes et al. [6,14] have reported the cavity-enhanced spontaneous emission of R6G in microdroplets of glycerol with diameters in the range 4–10 μm. The enhancement is predicted to be a function of the density of the cavity modes, depending on the position of the radiative dipole in the droplet, and hence the total emission decays observed are highly non-exponential, being characterized by a wide distribution of emission lifetimes ranging from the lifetime found in dilute bulk solution to a significantly shorter value.

In the present work, we report a time-resolved fluorescence study of the photodynamic processes of R6G at different concentrations, the energy transfer between the dye pair of R6G (donor) and malachite green (MG) (acceptor) and the fluorescence quenching of R6G by potassium iodide (KI), all in microdroplets of ethylene glycol. The combination of a mode-locked Ar^+ ion laser as excitation source and a fluorescence microscope to collect the fluorescence from droplets with diameters as small as 2 μm has enabled the effect of the droplet size on the electronic energy transfer from the donor to the acceptor to be investigated. A remarkable size effect on the Förster-type energy transfer has been observed in droplets with diameters of less than approximately 10 μm.

2. Experimental section

R6G (Exciton Laser grade), MG of a guaranteed grade (Aldrich Chemicals) and potassium iodide (KI) of a guaranteed grade (Waco Pure Chemical Industries, Ltd.) were used without further purification. Ethylene glycol of spectroscopic grade and silicone oil of 300 cSt (supplied by Kyoei Oil Co. Ltd.) were used as received. The following method was adopted for the preparation of droplets of R6G dissolved in ethylene glycol [9]. A small amount of ethylene glycol solution was dispersed in silicone oil by agitation using a magnetic stirrer. Since silicone oil and ethylene glycol are practically immiscible and R6G does not dissolve in silicone oil, the ethylene glycol solution containing R6G forms desirable small droplets of various sizes in silicone oil. After leaving the mixture to stand in order to allow the larger droplets to settle, the upper silicone layer containing the smaller droplets was sucked into a glass capillary (inner diameter, 200 μm). Both ends of the glass capillary were sealed with compound rubber, and the glass capillary was mounted on the stage of a Nicon XF-EFD epi-illumination fluorescence microscope for fluorescence decay measurements. The size of the droplet was measured with the microscope by using an objective micrometer. The uncertainty associated with the diameter measurements was estimated to be approximately 25% for the droplet of the smallest size. The refractive indices of ethylene glycol and silicone oil were measured with an Abbe refractometer model Atago 1T.

Fluorescence decay curves were measured using the time-correlated single-photon counting technique (TC-SPC) as described in detail elsewhere [10,15]. The excitation source was a Spectra Physics model 2016 Ar^+ ion laser mode locked at 514.5 nm. Fluorescence emission from a single droplet or a thin liquid film sample was detected with a Hamamatsu R928 photomultiplier tube mounted on the fluorescence microscope after passing it through a Toshiba O-54 cut-off glass filter inserted before the photomultiplier in order to remove the scattered excitation light. The diameter of the illuminated area was less than 10 μm. The laser intensity measured with a Newport model 835 power meter was less than 2.0 μW which was low enough not to cause lasing in the droplets. The magic angle for this system was determined experimentally by measuring the fluorescence decay from a thin liquid film of a dilute ethylene glycol solution of R6G sandwiched between a cover glass and a slide glass and by adjusting the orientation of the probe polarizer until a single exponential decay was recovered [9,15]. All of the fluorescence decay curves were measured under aerated conditions at room temperature with a channel width of 20.9 ps.

The measured fluorescence decay curves were analysed according to a single exponential function

$$I(t) = I(0) \exp(-t/\tau) \quad (1)$$

where τ is the best-fit single exponential decay time, or a non-exponential function given by

$$I(t) = I(0) \exp(-At - Bt^{1/2}) \quad (2)$$

using the technique of non-linear least-squares fitting discussed elsewhere [15,16]. The parameters A and B in Eq. (2) are defined in the text.

3. Results and discussion

3.1. Effect of droplet size on the fluorescence lifetime of R6G at low and high concentrations

The fluorescence decay curve of R6G, measured by a conventional method in a cuvette (path length, 1 cm), at concentrations greater than 1.0×10^{-6} M deviates from single exponential behaviour, and the apparent fluorescence lifetime obtained by best fitting to Eq. (1) increases with concentration due to the re-absorption effect as reported previously [16]. This distortion in the decay is undesirable and can be eliminated by using the technique of fluorescence microscopy where fluorescence is detected from a highly concentrated solution in a glass capillary (inner diameter, 20–200 μm) [17] or in a thin liquid film. After removing the re-absorption effect, the fluorescence lifetime of R6G in bulk solution is

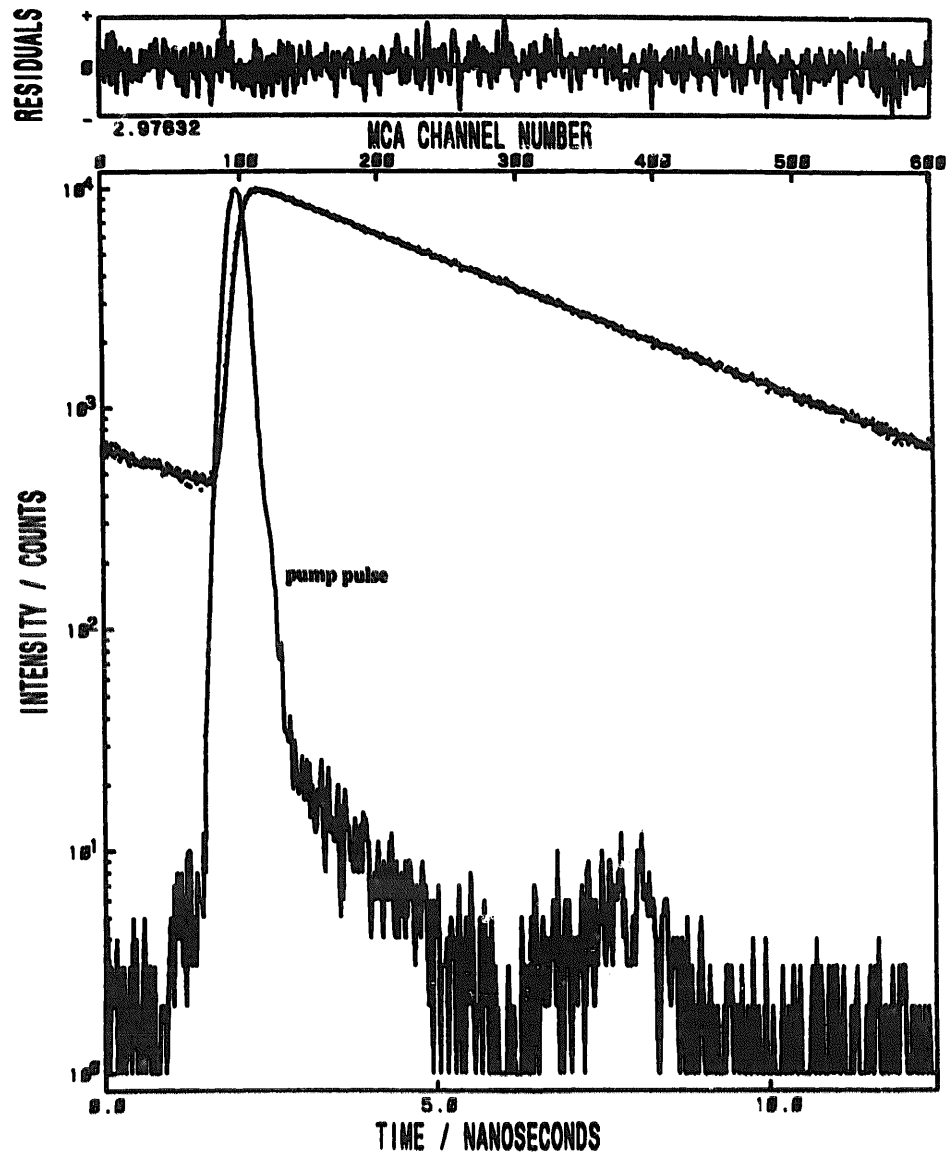

Fig. 1. Fluorescence decay curve (dots) measured for a thin liquid film of R6G in ethylene glycol (1.0×10^{-3} M). The full line is the best-fit single exponential function (Eq. 1) to the decay data. The distributions of the reduced residuals obtained for this analysis are also shown in the top panel.

expected to remain constant with concentration unless concentration quenching becomes appreciable [16,18].

Fig. 1 shows the fluorescence decay curve of highly concentrated R6G (1.0×10^{-3} M) in ethylene glycol measured in a glass capillary (inner diameter, 200 μm). The decay is exponential and the best-fit decay time ($\tau_f = 3.60 \pm 0.02$ ns) is equal to that obtained for a dilute solution (concentration, less than 1.0×10^{-6} M) contained in a 1 cm path length cuvette. The fluorescence decay of R6G measured in the thin glass capillary remains single exponential up to the highest concentration of 5.2×10^{-3} M used in the present work. The fluorescence lifetimes are distributed ($\Delta\tau = 0.05$ ns) around the intrinsic fluorescence lifetime of R6G (3.60 ns) measured at the lowest concentration. However, above 10^{-2} M, concentration quenching becomes appreciable and the apparent fluorescence lifetime rapidly decreases with concentration [18]. Therefore the concentration of R6G in the droplets was kept below this threshold value in this work.

The fluorescence lifetime of R6G is independent of the size of the droplet at low concentrations up to 1.0×10^{-4} M. This is in sharp contrast with the strong enhancement in the fluorescence decay rate and the non-exponentiality of the fluorescence decay observed by Barnes et al. [6,14] for R6G at very low concentration (1.0×10^{-6} M) in glycerol droplets with diameters of less than 10 μm. They used an electrodynamic trap to levitate the glycerol microdroplets and measured the fluorescence decay for a single droplet using TC-SPC. For droplets with diameters of less than 10 μm, the fluorescence decay was highly non-exponential and the decay rate increased sharply [6]. The decay rate of the major component was enhanced by a factor of ten in the 4 μm diameter droplet relative to that in bulk solution. These workers

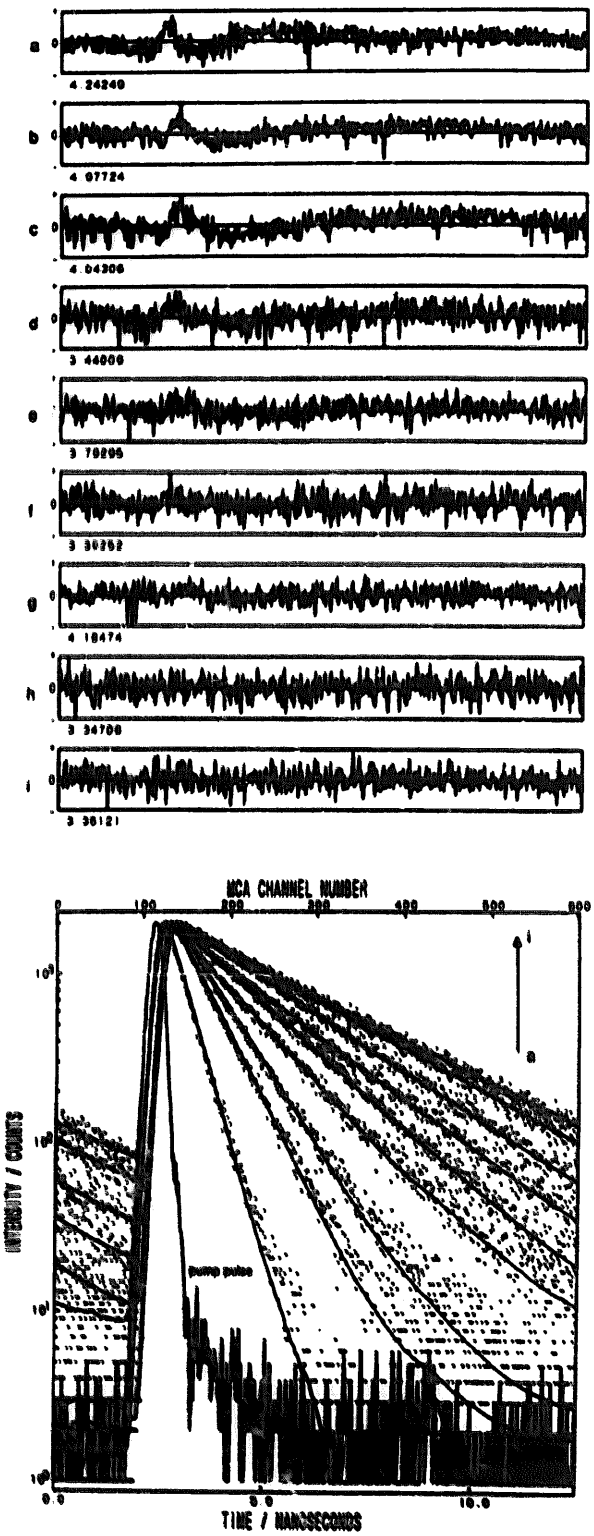

Fig. 2. Fluorescence decay data (dots) of R6G (5.2×10^{-3} M) for droplets of various diameters: (a) 2 μm; (b) 3 μm; (c) 4 μm; (d) 5 μm; (e) 7 μm; (f) 8 μm; (g) 9 μm; (h) 11 μm; (i) 14 μm. The full lines are the best-fit single exponential decay curves. The distributions of the reduced residuals corresponding to the analysis of the fluorescence decay curves (a)–(i) are shown in the top panels.

ascribed this enhancement in the fluorescence decay rate to cavity-enhanced spontaneous emission. We have not observed any such effect for ethylene glycol droplets of R6G with diameters in the range 2–20 μm at concentrations of 1.0×10^{-4} M or less.

At higher concentrations of R6G, however, the apparent fluorescence lifetime of R6G decreases with decreasing size of the droplet. This size dependence becomes quite significant at a concentration of 5.2×10^{-3} M. The fluorescence decay curves of R6G (5.2×10^{-3} M), fitted with single exponential functions, are shown in Fig. 2 for droplets of various diameters, together with the fluorescence decay of R6G in dilute bulk ethylene glycol solution. The distribution of the reduced residuals, corresponding to the analysis of the fluorescence decay curves using the exponential function given by Eq. (1), are shown in the top panels of Fig. 2. The fitting to Eq. (1) is satisfactory, enabling the apparent fluorescence lifetime to be defined by τ in Eq. (1). A large decrease in the counting rate of the emitted photons observed for small droplets indicates that the decrease in the fluorescence lifetime is not due to a change in the natural radiative lifetime τ_r or enhanced induced emission, but to fluorescence quenching.

Very efficient fluorescence quenching is observed for the smallest droplet. The apparent fluorescence lifetimes obtained at various concentrations of R6G are plotted as a function of the droplet diameter in Fig. 3. At a concentration of 1.0×10^{-4} M, the decay time remains practically unchanged with droplet size. At higher concentrations of R6G, the fluorescence decay time decreases as the diameter of the droplet decreases and the size effect becomes more significant at higher concentrations. It is also interesting to note that the fluorescence decay remains almost single exponential even for droplets of the smallest size (2 μm) for which the decay time is decreased by approximately a factor of ten, i.e. from 3.60 ns to 0.4 ns. Here, it should be mentioned that only 1000 or 2000 counts were accumulated in the channel of maximum intensity, which is due to the fact that the apparent fluorescence lifetime of R6G in small droplets is influenced by prolonged laser irradiation. This aspect is discussed in detail in Section 3.2.

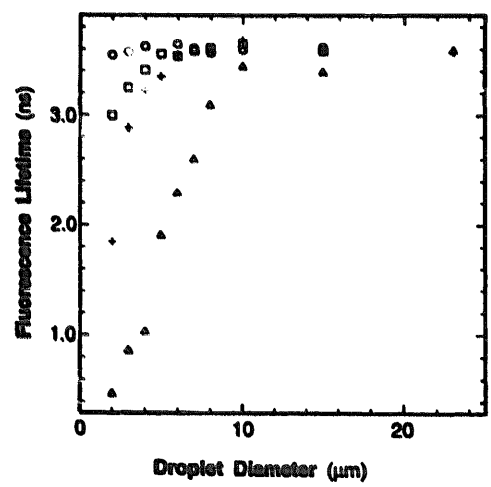

Fig. 3. Plot of the fluorescence lifetime of R6G vs. the diameter of the droplet. The concentrations of R6G are 1.0×10^{-4} M (○), 1.0×10^{-3} M (□), 2.0×10^{-3} M (+) and 5.2×10^{-3} M (△).

The size effect on the apparent fluorescence lifetime of R6G observed at higher concentrations cannot be explained on the basis of a change in concentration of the dimer, which is formed appreciably in highly concentrated solutions and can act as a trapping centre for excited monomer molecules [19]. The equilibrium between the monomer and dimer may be influenced by the droplet size. Indeed, the slight decrease in the fluorescence lifetime with decreasing droplet size, reported for ethylene glycol droplets of rhodamine B in Ref. [9], was explained by an increase in the dimer concentration. However, in the present case, the concentration of the dimer should increase by approximately tenfold in order to account for the observed shortening. Such a large increase in the dimer concentration in the droplets is very unlikely. Some other reason must be responsible for the observed enhancement in the fluorescence quenching as discussed in Section 3.3.

3.2. *Effect of laser irradiation*

The fluorescence decay features of R6G in droplets with small diameters are affected by laser irradiation at 514.5 nm. Fig. 4 shows the effect of laser irradiation on the fluorescence decay of R6G (5.3×10^{-3} M) in droplets of 2 μm in diameter. The distributions of the reduced residuals, corresponding to the analysis of the decay curves, are given in the top panels of Fig. 4. It can be seen from Fig. 4 that an increase in the laser irradiation time leads to an increase in the apparent fluorescence lifetime of R6G. As a result of this change, the fluorescence decay becomes highly non-exponential when a larger number of emitted photons are accumulated by continued laser irradiation, since a number of emission decays with different lifetimes become superimposed. In order to avoid this distortion in the decay curve, only 1000 or 2000 counts were accumulated in the channel of maximum intensity, for which the fluorescence decay was distinctly single exponential. The apparent fluorescence lifetime of R6G increases from 0.4 ns to 2.7 ns after about 90 min of laser irradiation, while the fluorescence decay remains single exponential throughout the measurements. However, further prolonged irradiation leads to a decrease in the fluorescence lifetime and results in a non-exponential decay.

The increase in the apparent fluorescence lifetime of concentrated R6G in the droplet on laser irradiation was puzzling at the early stage of this work, but can now be explained consistently on the basis of a decrease in the concentration of the dimer. Laser irradiation causes the photodegradation of R6G [13] which reduces not only the concentration of the R6G monomer, but also the dimer, which is in equilibrium with the monomer and acts as a trapping centre. Thus energy migration between the monomer molecules, as well as trapping by the dimer, becomes less frequent with photodegradation, resulting in less efficient fluorescence quenching and hence in an increase in the apparent fluorescence lifetime. If any photoproduct which emits in the observation wavelength range (550 nm or above) is responsible for the increase, the fluorescence decay should assume some non-exponentiality

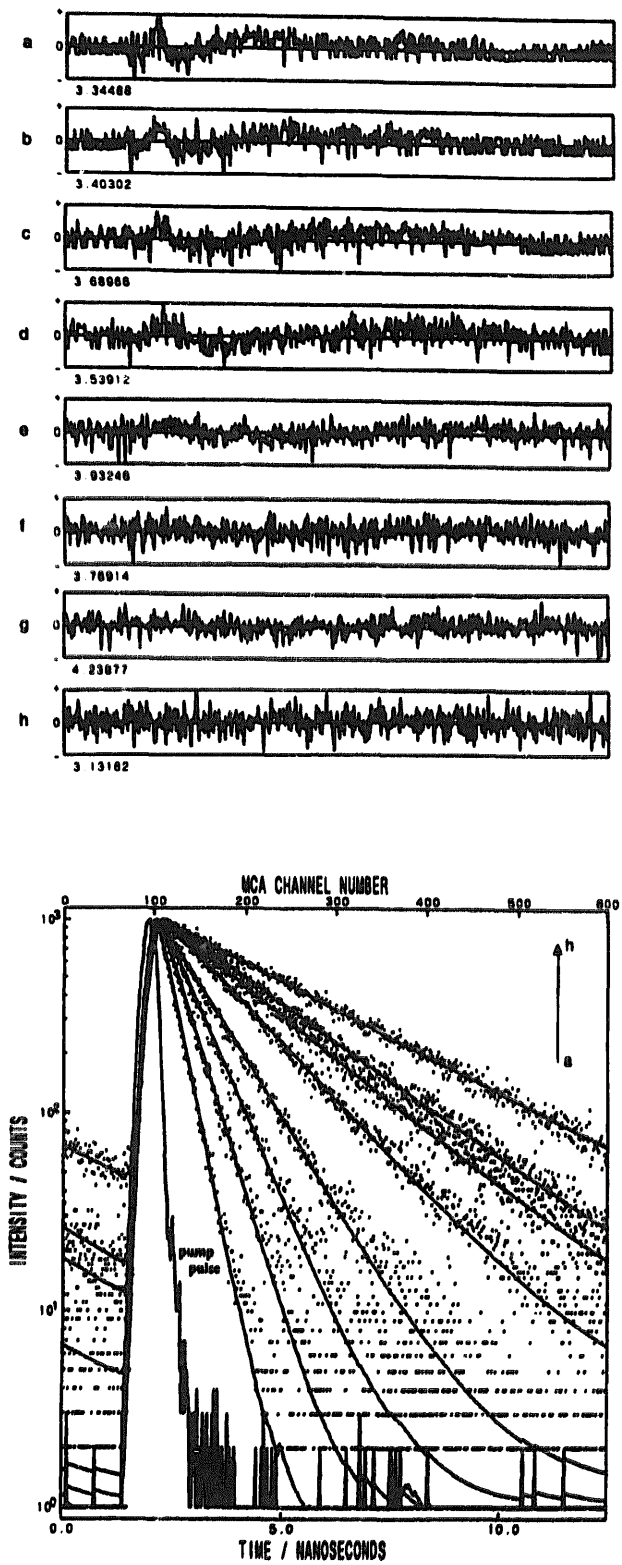

Fig. 4. Fluorescence decay of R6G (5.2×10^{-3} M) showing the effect of laser irradiation on the 2 μm droplet. The decay curves were measured after pre-illumination of 0 min (a), 5 min (b), 10 min (c), 15 min (d), 35 min (e), 60 min (f) and 90 min (g). Curve (h) is the decay curve of the bulk solution of R6G measured in a thin glass capillary at the same concentration. The full lines are the best-fit single exponential decay curves. The distributions of the reduced residuals corresponding to the analysis of the fluorescence decay curves (a)–(h) are shown in the top panels.

even when measured at low count numbers of the emitted photons.

3.3. R6G to MG energy transfer in the droplets

The transfer of excitation energy from R6G to MG in bulk solutions has been investigated by many workers [18,20,21]. Scully et al. [18] have extensively investigated this system in ethylene glycol and have found that excitation energy transfer can be described by the Förster model [22] under static conditions of low donor and high acceptor concentrations, whereas the Loring–Anderson–Fayer (LAF) model [23] is more appropriate to explain the effect of excitation migration and transfer in the high donor concentration regime.

The fluorescence decay curve of R6G measured at a concentration of 1.0×10^{-4} M in the presence of MG becomes non-exponential, and can be described by the Förster model of energy transfer given by Eq. (2) in which

$$\left.\begin{aligned} A &= \tau_0^{-1} \\ B &= \gamma(4/3)\pi^{3/2}\rho_A(R_0^{DA})^3\tau_0^{-1/2} \end{aligned}\right\} \quad (3)$$

where τ_0 is the unquenched fluorescence lifetime of the excited donor, γ is the numerical factor given by $(3/2\langle\kappa^2\rangle)^{1/2}$ and $\langle\kappa^2\rangle$ is the averaged orientation factor. In the "dynamic averaging limit", molecular reorientation is infinitely rapid, $\langle\kappa^2\rangle = 2/3$ and hence γ has a value of unity. In the static averaging limit, the orientation is fixed throughout the energy transfer and the value of γ is calculated to be 0.846 [24]. ρ_A is the acceptor number density and R_0^{DA} is the critical energy transfer distance at which the rates of non-radiative energy transfer and intrinsic deactivation of the donor are of equal probability. The value of R_0^{DA} can be calculated from the spectral overlap between the emission spectrum of the donor and the absorption spectrum of the acceptor molecule by the following equation [24]

$$(R_0^{DA})^6 = \frac{9000\ln(10)\kappa^2\phi_0}{128\pi^5 n^4 N}\int_0^\infty \frac{F_D(\bar{\nu})\epsilon_A(\bar{\nu})}{\bar{\nu}^4}\,d\bar{\nu} \quad (4)$$

where ϕ_0 is the fluorescence quantum yield of the unquenched donor, $F_D(\bar{\nu})$ is the spectral distribution of the donor emission in quanta normalized to unity, $\epsilon_A(\bar{\nu})$ is the decadic molar extinction coefficient of the acceptor at the wavenumber $\bar{\nu}$ and n is the refractive index of the solvent.

Fig. 5 shows the fluorescence decay data of bulk solutions of R6G (1.0×10^{-4} M) in the presence of various concentrations of MG (5.0×10^{-4}–2.0×10^{-3} M) in a thin glass capillary, fitted with the Förster function of Eq. (2). The quality of fitting can be seen from the residuals shown in the top panel of the figure. The residuals corresponding to the fitting of the same data to a single exponential function (Eq. (1)) are also shown in the bottom panels for comparison. The values of R_0^{DA} calculated from the fitted values of A and B are in good agreement with the value of 5.9 nm calculated spectroscopically using Eq. (4).

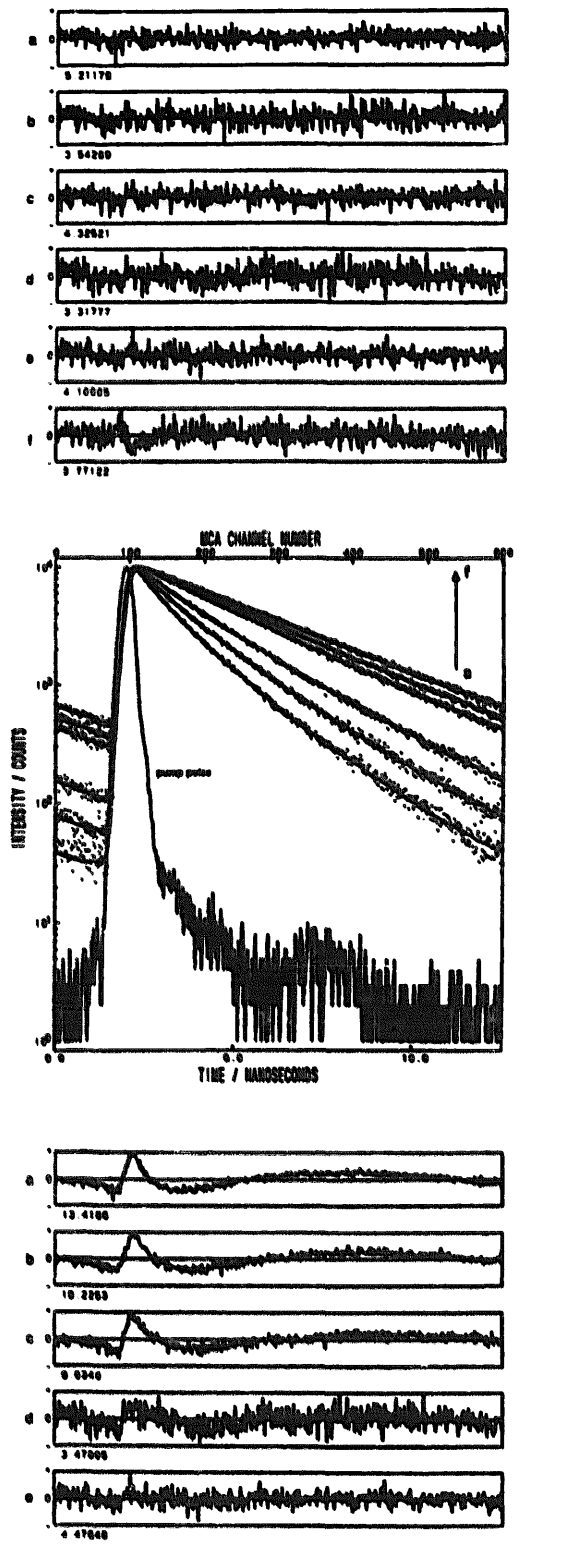

Fig. 5. Fluorescence decay data (dots) measured for a thin film of ethylene glycol containing R6G (1.0×10^{-4} M) and MG. The concentrations of MG are 2.0×10^{-3} M–1.0×10^{-4} M in curves (a)–(e). The full lines are the best-fit decay curves calculated using the Förster function (Eq. 2) to the data points. Curve (f) is the single exponential decay of R6G in the absence of MG. The distributions of the residuals corresponding to the analysis of the decay curves (a)–(f) are shown in the top panels. The distributions of the reduced residuals obtained by fitting the same data points ((a)–(e)) to single exponential functions are also shown in the bottom panels for comparison.

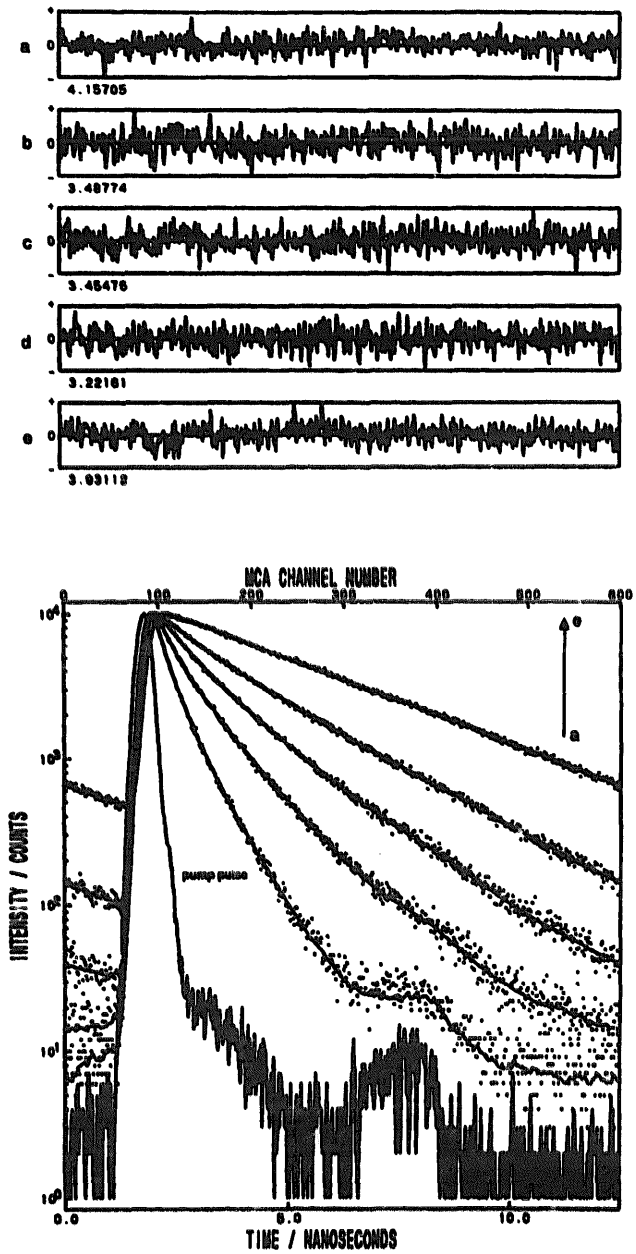

Fig. 6. Decay curves showing the size effect on the fluorescence decay of R6G (1.0×10^{-4} M) in the presence of MG (7.5×10^{-4} M). The diameters of the droplets are 2 μm (a), 3 μm (b) and 5 μm (c). Curve (d) is the fluorescence decay curve of the bulk solution. The full lines are the best-fit curves of the decay data to Eq. 2. The distributions of the residuals corresponding to the analysis of the decay curves (a)–(e) are shown in the top panels. The fluorescence decay curve of pure R6G (1.0×10^{-4} M) fitted to a single exponential is also shown (curve (e)).

A very significant enhancement in the energy transfer is observed in droplets of smaller diameter. Fig. 6 and Fig. 7 show the fluorescence decay curves of R6G (1.0×10^{-4} M) in the presence of MG at two different concentrations (7.5×10^{-4} M and 2.0×10^{-3} M) in ethylene glycol droplets with various diameters. The fluorescence decay of the bulk mixture in the thin glass capillary is also shown for comparison. The fluorescence decay curve measured for droplets with diameters larger than 10 μm is essentially the same as that observed for the bulk solution in the thin glass capillary. It can be seen that the quenching efficiency due to energy transfer increases significantly as the droplet diameter decreases. The decay curves were fitted to Eq. (2) and the best-fit values for parameters A and B at the three concentrations of the acceptor are given in Table 1.

It can also be seen from the random distribution of the residuals that the Förster model holds reasonably well for droplets of all diameters examined, although increasing parameter A values (see Table 1) with decreasing diameter

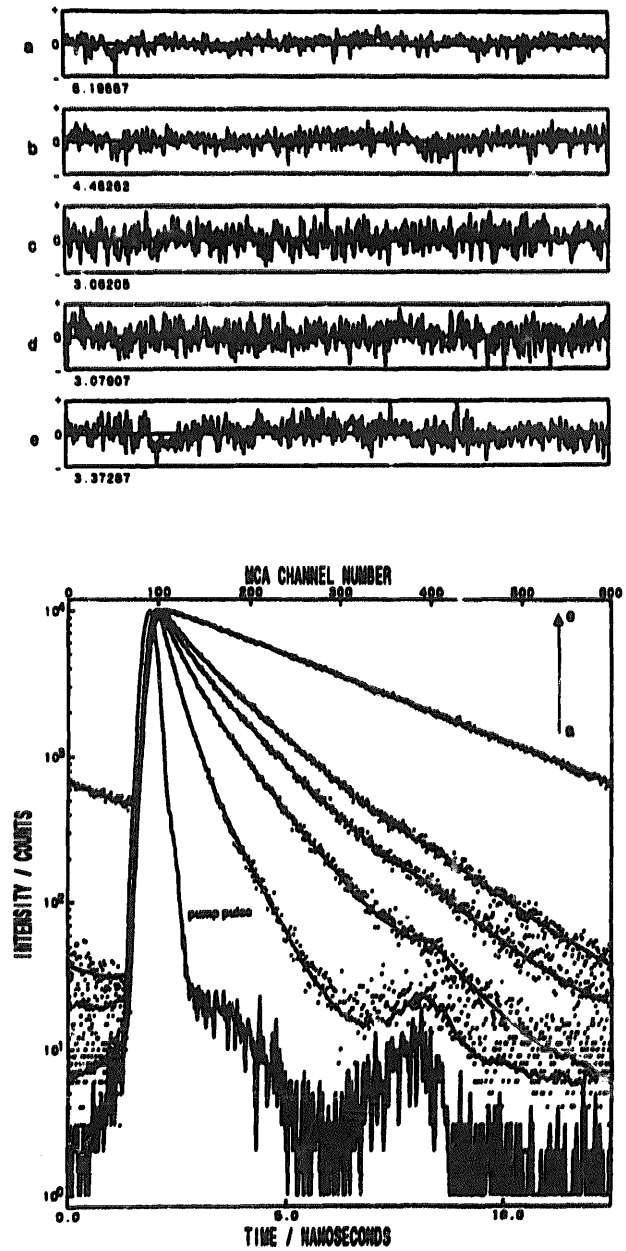

Fig. 7. Size effect on the fluorescence decay curve of R6G (1.0×10^{-4} M) in the presence of MG (2.0×10^{-3} M). The diameters of the droplets are 3 μm (a), 4 μm (b) and 8 μm (c). Curve (d) is the fluorescence decay measured for the bulk solution at the same concentration. The full lines are the best-fit curves of the decay data to Eq. 2. The fluorescence decay curve of pure R6G (1.0×10^{-4} M) fitted to a single exponential is also shown (curve (e)). The distributions of the residuals corresponding to the analysis of the decay curves (a)–(e) are shown in the top panels.

Table 1
Results of the analysis of the fluorescence decay curves measured for ethylene glycol droplets of donor (R6G) and acceptor (MG) using the Förster model (Eq. 2). The concentration of R6G is 1.0×10^{-4} M

Concentration of MG ($\times10^{3}$ M)	Diameter of droplet (μm)	A (ns^{-1})	B ($ns^{-1/2}$)	R_0^{DA} (nm)
0.75	Bulk	0.301	0.316	5.90
	10	0.299	0.314	5.89
	8	0.306	0.320	5.93
	5	0.310	0.601	7.32
	4	0.331	0.705	7.72
	3	0.351	1.01	8.69
	2	0.409	2.01	10.9
1.0	Bulk	0.319	0.427	5.93
	17	0.323	0.426	5.92
	5	0.322	0.822	7.37
	4	0.349	0.898	7.59
	3	0.402	1.43	8.87
	2	0.477	2.48	10.7
2.0	Bulk	0.368	0.835	5.88
	30	0.369	0.935	6.11
	10	0.377	1.14	6.53
	8	0.398	1.25	6.75
	5	0.446	1.54	7.21
	3	0.552	2.90	8.91

Table 2
Results of the analysis of the fluorescence decay curves measured for ethylene glycol droplets of donor (R6G) and quencher (KI) using Eq. 4. The concentration of R6G is 1.0×10^{-4} M

Concentration of KI (M)	Diameter of droplet (μm)	α (ns^{-1})	β ($ns^{-1/2}$)	R (nm)
0.25	Bulk	0.415	0.405	0.79
	5	0.537	0.773	0.99
	3	0.605	0.813	0.94
	2	0.637	0.946	1.01

of the droplet suggest a slight deviation from this theory which predicts a constant value for A of τ_0^{-1}. Here, it is important to point out that the fluorescence decay of pure R6G at this concentration (1.0×10^{-4} M) shows no size effect (see Fig. 3). It can be seen from Table 1 that the value of parameter B for the droplet of smallest diameter is increased approximately five times compared with that in the bulk solution. In other words, the apparent value of the critical transfer distance, R_0^{DA}, calculated from the best-fit values of B using Eq. (3), at the smallest diameter examined in this work is approximately twice the value obtained for the bulk solution. If it is assumed that the concentrations of the donor and acceptor molecules remain constant as the size of the droplet decreases, this means that the rate constant for energy transfer at a given distance, $k_{DA}=(1/\tau_0)(R_0^{DA}/R)^6$, increases by a factor of 2^6. Such an enhancement in the energy transfer rate can be ascribed to an increase in the dipole–dipole interaction in microdroplets [8], since the quenched fluorescence decay data always follow the Förster function (Eq. (2)) for droplets of all diameters examined, as is evident from the quality of fitting for various droplet sizes.

Another point to be noted from Table 1 is that, although the energy transfer efficiency increases with decreasing diameter of the droplet, the overall increase in the transfer efficiency for a droplet of a particular diameter, compared with that of the bulk solution, is almost the same for all acceptor concentrations. It can also be seen from Table 1 that the effective value of the critical transfer distance is independent of the acceptor concentration for a droplet of a particular size, although the rate of energy transfer increases with acceptor concentration, as is evident from the increasing values of B. The remarkable size effect observed on the decay rate of R6G at high concentrations, as described in Section 3.1, can be explained in terms of the enhanced rate of excitation migration in droplets of smaller size. At high concentrations of R6G, the process of excitation migration becomes dominant. The rate of excitation migration via dipole–dipole interaction, $k_{DD}=(1/\tau_0)(R_0^{DD}/R)^6$ (where R_0^{DD} is the critical transfer distance for excitation migration), increases rapidly as the droplet size decreases leading to enhanced trapping by dimers. The energy migration is so efficient that the quenched decay curves assume almost single exponential decays as shown in Fig. 2 [25].

3.4. Fluorescence quenching of R6G by KI in the droplets

The significant size effect observed for the fluorescence quenching of R6G by MG through energy transfer was not

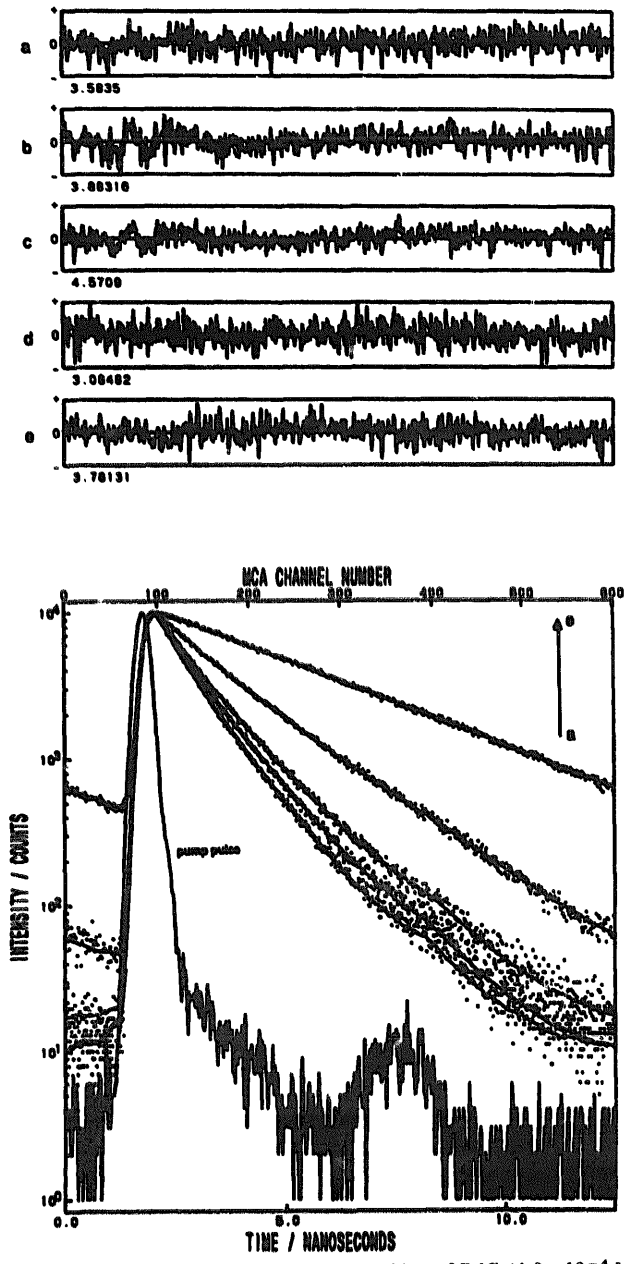

Fig. 8. Size effect on the fluorescence quenching of R6G (1.0×10^{-4} M) by KI (0.25 M). The diameters of the droplets are 2 μm (a), 3 μm (b) and 5 μm (c). The full lines are the best-fit curves of the decay data to a non-exponential function (Eq. 4). The fluorescence decay curve of pure R6G (1.0×10^{-4} M) fitted to a single exponential is also shown (curve (e)). The distributions of the residuals corresponding to the analysis of the decay curves (a)–(e) are shown in the top panels.

observed for the quenching of R6G by KI. Fig. 8 shows the effect of size on the fluorescence quenching of R6G (1.0×10^{-4} M) by KI (0.25 M). The decay data were fitted to a non-exponential function, which is associated with the long-time approximation to the equation derived from the Smoluchowski–Collins–Kimball (SCK) model [26]

$$\left.\begin{aligned} I(t) &= I(0)\exp(-\alpha t-\beta t^{1/2}) \\ \alpha &= \tau_0^{-1}+4\pi RDN[\mathrm{Q}] \\ \beta &= 8(\pi D)^{1/2}R^2N[\mathrm{Q}] \end{aligned}\right\} \quad (5)$$

whose functional form is coincidentally the same as that of Eq. (2). However, the parameters α and β are defined differently from A and B in Eq. (2). τ_0 is the unquenched fluorescence lifetime of the electronically excited fluorophore, D is the sum of the diffusion coefficients of the two reactants, N is Avogadro's number, [Q] is the quencher concentration and R is the apparent reaction distance. The best-fit values for parameters α and β and the values for R calculated from these best-fit values are given in Table 2.

It can be observed that, although the quenching rate increases in droplets of smaller diameter, the effect is not as remarkable as in the case of the quenching of R6G fluorescence by MG via long-range energy transfer. In fact, the values of R increase only slightly with decreasing droplet size. The mechanism of fluorescence quenching of R6G by KI involves electron transfer which occurs exclusively at an encounter distance of approximately 1.0 nm [27]. This result suggests that short-range electron transfer is not as strongly enhanced as long-range energy transfer mediated by dipole–dipole interaction.

3.5. Size effect on the photodynamic processes

The electromagnetic field generated in small dielectric spheres, such as aerosols or microdroplets, is strongly dependent on the size of the sphere and the frequency of the electromagnetic wave [11,12,28]. Druger et al. [8] have shown that, when acceptor and donor molecules are present in a droplet, the coupling of the enhanced electromagnetic field with the donor and acceptor transition dipoles can enhance significantly the efficiency of energy transfer from the donor to the acceptor. According to their predictions, the energy transfer is enhanced by more than 100 times in droplets with diameters as large as 10 μm. However, this enhancement is a strong function of the radius at a fixed frequency and is only observed in the peripheral shell whose volume is approximately 15% of the total volume of the sphere. They also estimated the effect of the droplet size on the radiative lifetime, and concluded that there is only a marginal effect on the radiative lifetime of a given fluorophore in a small dielectric sphere. They ascribed this insensitive nature of the radiative lifetime to the droplet size to the off-range interaction. On the other hand, Gersten and Nitzan [12] predicted an oscillating nature of the radiative lifetime in their general discussion of the size effect on the radiative lifetime. According to them, the radiative process is enhanced by more than 10 times under certain circumstances [12]. Barnes et al. [6,14] recently reported a significant decrease in the fluorescence lifetime of R6G in microdroplets levitated in vacuum, as well as a significant distribution of the fluorescence lifetimes, suggesting that the enhancement in the radiative process is only observed for the peripheral shell of these droplets.

The results obtained in this work are for droplets with practically no dielectric interface, and hence cannot be explained on the basis of any of the existing theoretical models [8,29]. It is not the purpose of this work to develop a new theory, but the theory to be developed should be able to rationalize a significant enhancement in the rate of Förster-type energy transfer without any measurable size effect on the natural radiative lifetime of the donor molecule. The theory should be able to explain quantitatively the following points.

1. The size at which the enhancement in energy transfer is seen. In our case, enhancement was not observed for droplets with diameters larger than 10 μm, as shown in Fig. 6. When a dielectric interface exists for droplets, such as those levitated in vacuum, the theory based on morphology-dependent resonance (MDR) predicts that the enhanced energy transfer will extend over distances of tens of micrometres [8]. On the other hand, no enhancement in the energy transfer will be seen unless a dielectric interface exists. Our droplets are immersed in a dielectric medium (silicone oil) and there is not much difference in the refractive indices (Δn) of silicone oil ($n = 1.4140$) and ethylene glycol ($n = 1.4318$). In spite of this, an enhancement in energy transfer was observed. The present findings are important since droplets dispersed in condensed media have more relevance to biological phenomena than droplets levitated in vacuum.
2. The active shell. The MDR-mediated enhanced energy transfer (or radiative process) is observed only in an active shell near the surface of the droplet, occupying less than 15% of the total volume of the droplet [8,14]. If the enhancement in energy transfer is restricted to only a small peripheral volume of the droplet, the emission decay curve measured from the whole droplet should assume appreciable non-exponentiality because of the superimposition of more than two decay curves with largely different decay rates. In the present work, all of the measured emission decays were satisfactorily described by either a single $t^{1/2}$ function (Eq. (2) or Eq. (5)) or a single exponential function (Eq. (1)). Therefore it appears that the enhanced energy transfer reported in this work prevails over the whole volume of the droplet irrespective of the droplet size.

An advantage of measuring the fluorescence decay curves is that these measurements make it feasible to compare the experimental results with the theory quantitatively. The knowledge of the emission decay features for microdroplets is still limited and the accumulation of such data for droplets with and without a dielectric interface is desirable in order to achieve a more quantitative comparison of experimental results with theory in future.

4. Conclusions

1. At low concentrations (1.0×10^{-4} M or less), the fluorescence decay from R6G shows practically no dependence on the droplet size, indicating that the radiative process and the intramolecular radiationless process are unaffected by a decrease in the droplet size to 2 μm in diameter.
2. R6G shows a large size effect on the fluorescence decay at higher concentrations (1.0×10^{-3} M or more). The sharp decrease in the apparent fluorescence lifetime in the smaller droplets at high concentration can be explained on the basis of enhanced energy transfer via energy migration between monomer molecules, followed by energy trapping by the dimer which acts as a quenching centre. Energy migration is so efficient that the quenched decay curves assume almost single exponential decays.
3. The long-range energy transfer from R6G to MG shows a significant enhancement at droplet sizes of less than 10 μm in diameter, whereas the quenching of R6G by KI via short-range electron transfer exhibits only a small size effect.

Acknowledgements

The authors wish to express their sincere thanks to K. Nakamura for his help in the preparation of the microdroplets and for fluorescence microscopy measurements. K.K.P. is grateful for financial support from the Japanese Ministry of Education, Science and Culture (Monbusho) during his stay at the Kyoto Institute of Technology. S.H. is grateful for financial support from the Japanese Ministry of Education, Science and Culture (Grants-in-Aid 04215103 and 03640407).

References

[1] A.J. Campillo and H.-B. Lin, in P.W. Barber and R.K. Chang (eds.), *Optical Effects Associated with Small Particles*, World Scientific, Singapore, 1988, Chapter 3.
[2] I. Colbeck, in D.J. Wedlock (ed.), *Controlled Particle, Droplet and Bubble Formation*, Butterworth Heinemann, Oxford, 1994.
[3] S.-X. Qian, J.B. Snow, H.M. Treng and R.K. Chang, *Science, 231* (1986) 486.
[4] L.M. Folan, S. Arnold and S.D. Druger, *Chem. Phys. Lett., 118* (1985) 322.
[5] S. Arnold and L.M. Folan, *Opt. Lett., 14* (1989) 3387.
[6] M.D. Barnes, W.B. Whitten, S. Arnold and J.M. Ramsey, *J. Chem. Phys., 97* (1992) 7842.
[7] W.B. Whitten, J.M. Ramsey, S. Arnold and B.V. Bronk, *Anal. Chem., 63* (1991) 1027.
[8] S.D. Druger, S. Arnold and L.M. Folan, *J. Chem. Phys., 87* (1987) 2649.
[9] M. Kawahigashi and S. Hirayama, *J. Lumin., 43* (1989) 207.
[10] S. Hirayama, in J.F. Rabek (ed.), *Progress in Photochemistry and Photophysics*, Vol. VI, CRC Press, 1992, p. 1.
[11] H.-B. Lin, J.D. Eversole, C.D. Merritt and A.J. Campillo, *Phys. Rev. A, 45* (1992) 6756.
[12] J. Gersten and A. Nitzan, *J. Chem. Phys., 95* (1991) 686.
[13] M.D. Barnes, K.C. Ng, W.B. Whitten and J.M. Ramsey, *Anal. Chem., 65* (1993) 2360.

[14] M.D. Barnes, W.B. Whitten and J.M. Ramsey, *Chem. Phys. Lett.*, *227* (1994) 628.
[15] T. Minami, M. Kawahigashi, Y. Sakai, K. Shimamoto and S. Hirayama, *J. Lumin.*, *35* (1986) 247.
[16] Y. Sakai, M. Kawahigashi, T. Minami, T. Inoue and S. Hirayama, *J. Lumin.*, *42* (1989) 317.
[17] K. Nakamura, *M.Sc. Thesis*, Kyoto Institute of Technology, 1994.
[18] A.D. Scully, M. Matsumoto and S. Hirayama, *Chem. Phys.*, *157* (1991) 253.
[19] A. Penzkofer and Y. Lu, *Chem. Phys.*, *103* (1986) 399.
[20] R.J.D. Miller, M. Pierre and M.D. Fayer, *J. Chem. Phys.*, *78* (1983) 5138.
[21] G. Porter and C.J. Tredwell, *Chem. Phys. Lett.*, *56* (1978) 278.
[22] Th. Förster, *Z. Naturforsch., Teil A*, *4* (1949) 321.
[23] R.F. Loring, H.C. Anderson and M.D. Fayer, *J. Chem. Phys.*, *76* (1982) 2015.
[24] D.P. Miller, R.J. Robbins and A.H. Zewail, *J. Chem. Phys.*, *75* (1981) 3649.
[25] D.L. Huber, *Phys. Rev. B*, *20* (1979) 2307.
[26] S.A. Rice, in C.H. Bamford, C.F.H. Triper and R.G. Compton (eds.), *Comprehensive Chemical Kinetics, Vol. 25, Diffusion-Limited Reactions*, Elsevier, Amsterdam, 1985.
[27] N. Periasamy, S. Doraiswamy, G.B. Maiya and B. Venkataraman, *J. Chem. Phys.*, *88* (1988) 1638.
[28] C.F. Bohren and D.R. Huffman, *Absorption and Scattering of Light by Small Particles*, Wiley-Interscience, New York, 1983.
[29] P.T. Leung and K. Young, *J. Chem. Phys.*, *89* (1988) 2894.